Achromobacter xylosoxidans modulates Pseudomonas aeruginosa virulence through a complex multi-target competition

Alison Besse, Quentin Menetrey, Vincent Jean-Pierre, Sylvaine Huc-Brandt, Fabien Aujoulat, Chloé Dupont, Raphaël Chiron, Jean Armengaud, Estelle Jumas-Bilak, Virginie Molle, et al.

scientific reports

Check for updates

OPEN

Achromobacter xylosoxidans modulates *Pseudomonas aeruginosa* virulence through a complex multi-target competition

Alison Besse[1,10]✉, Quentin Menetrey[2,10], Vincent Jean-Pierre[3], Sylvaine Huc-Brandt[4], Fabien Aujoulat[1], Chloé Dupont[5], Raphaël Chiron[6], Jean Armengaud[7], Estelle Jumas-Bilak[8], Virginie Molle[9], Lucia Grenga[7] & Hélène Marchandin[3]

The colonization and persistence of *Pseudomonas aeruginosa* in chronically diseased lungs are driven by various virulence factors. However, pulmonary infections in cystic fibrosis (CF) patients are predominantly polymicrobial. While *Achromobacter xylosoxidans* is an opportunistic pathogen in these patients, its impact on *P. aeruginosa* virulence during co-infection remains largely unknown. This study investigated *P. aeruginosa* interaction with two clonally related *A. xylosoxidans* strains, Ax 198 and Ax 200, co-isolated from CF sputum. We found that the interaction was strain-dependent, with Ax 200 significantly reducing *P. aeruginosa* virulence in a zebrafish model, providing the first *in vivo* evidence of this interaction. Proteomic analysis revealed that *P. aeruginosa* proteome was differently impacted by the two *A. xylosoxidans* strains, with Ax 200 altering proteins involved in biofilm formation, swimming motility, iron acquisition, and secretion systems. These findings were validated by phenotypic assays, confirming that *A. xylosoxidans* affected major *P. aeruginosa* virulence phenotypes, including biofilm formation, swimming motility, and siderophore production. Genetic analysis confirmed that distinct regulatory mechanisms, including iron cycle pathways, may account for the strain-dependent effects. These findings reveal a novel multi-target competitive mechanism through which *A. xylosoxidans* significantly disrupts *P. aeruginosa* virulence.

Keywords *P. aeruginosa*, Inter-bacterial interaction, Virulence, Cystic fibrosis, *A. xylosoxidans*

Pseudomonas aeruginosa (Pa) is ubiquitous in moist environments like water and soil[1,2], and is a leading pathogen in healthcare-associated infections[3–6]. Pa is also a major cause of lung infection in people with cystic fibrosis (CF)[7]. Colonization and persistence of Pa within chronically diseased lungs is driven by the production of virulence factors, such as biofilm formation with increased exopolysaccharide (EPS) production; quorum sensing (QS); motility and attachment involving flagella, type IV pili (T4P) and lectins; secretion systems (TSSs); production of pyocyanin and rhamnolipids; and iron acquisition systems[8]. However, pulmonary infections in CF patients are predominantly polymicrobial[9,10], with the two major pathogens, Pa and *Staphylococcus aureus*, alongside other species such as *Achromobacter xylosoxidans* (Ax), which are increasingly recognized as opportunistic CF pathogens[7,11]. Although co-isolation of Ax and Pa has been reported[12–14], inter-species interaction has rarely been studied, and the impact of Ax on Pa virulence during co-infection remains largely unknown. So far, only two studies have reported *in vitro* interaction between Pa and Ax, including our own previous work[13,14].

[1]HydroSciences Montpellier, Univ Montpellier, CNRS, IRD, Montpellier, France. [2]INFINITE-Institute for Translational Research in Inflammation, Univ Lille, INSERM, Lille, France. [3]HydroSciences Montpellier, Univ Montpellier, CNRS, IRD, Service de Microbiologie et Hygiène Hospitalière, CHU Nîmes, Montpellier, France. [4]Laboratory of Pathogens and Host Immunity (LPHI) UMR5294, University of Montpellier, CNRS, INSERM, Montpellier, France. [5]MIVEGEC, IRD, CNRS, Univ Montpellier, Laboratoire de Bactériologie, CHU Montpellier, Montpellier, France. [6]HydroSciences Montpellier, Univ Montpellier, CNRS, IRD, Centre de Ressources et de Compétences de la Mucoviscidose, CHU Montpellier, Montpellier, France. [7]Université Paris-Saclay, Département Médicaments et Technologies pour la Santé, CEA, INRAE, SPI, 30200 Bagnols-sur-Cèze, France. [8]HydroSciences Montpellier, Univ Montpellier, CNRS, IRD, Laboratoire d'Écologie Microbienne Hospitalière, CHU Montpellier, Montpellier, France. [9]VBIC, INSERM U1047, University of Montpellier, Montpellier, France. [10]These authors contributed equally: Alison Besse and Quentin Menetrey. ✉email: alison.besse@umontpellier.fr

We already demonstrated that interactions between Pa and Ax strain pairs significantly inhibited Pa growth, swimming motility, and pigment production[13]. In addition, Sandri *et al.* reported cases of either competition or coexistence between strains of these two species[14]. Yet, the molecular basis underlying the interaction between them remain unexplored. Furthermore, no *in vivo* studies have addressed how this interaction influences Pa virulence, leaving a critical gap in our understanding of the dynamics of these co-infections.

Based on our previous work, we selected a Pa (Pa II.17) and two Ax strains (Ax 198 and Ax 200), co-isolated from a CF sputum sample. Among these, the Pa II.17 and Ax 200 pair showed the strongest competitive interactions, while the Pa II.17 and Ax 198 pair had a noticeably weaker effect on Pa virulence factors *in vitro*[13]. The aim of this study is to (i) validate *in vivo* previous *in vitro* observations suggesting that the virulence of Pa is reduced in the presence of Ax, (ii) uncover the molecular basis involved in the significant reduction of Pa virulence, and (iii) explore why strains of Ax exhibit varying capacities to competitively inhibit Pa virulence.

Results

Genomic similarity between *A. xylosoxidans* co-isolated strains Ax 198 and Ax 200

The genomes of Ax 198 and Ax 200 were found to have very similar lengths (6.55 Mb). The two Ax genomes also showed 99.98% and 99.90% of similarity, according to average nucleotide identity based on BLAST and digital DNA-DNA hybridization respectively (Fig. S1); indicating their clonality and supporting the idea that they represent two adaptive variants of the Ax strain colonizing the patient.

A. xylosoxidans Ax 200, but not Ax 198, reduces *P. aeruginosa* virulence in a zebrafish infection model

First, we assessed the suitability of the zebrafish bath infection model to evaluate Pa-Ax interactions *in vivo* by examining the survival of zebrafish infected with Pa II.17. A dose-dependent relationship between Pa II.17 and zebrafish mortality was observed, with approximately 20% mortality observed at a low dose 30 h post-infection (hpi), while 100% mortality occurred at the highest dose within 22 hpi (Fig. 1A), confirming that this is a robust experimental system for studying Pa virulence. On the other hand, both Ax 200 and Ax 198 (suspension at $OD_{600} = 0.5$) were avirulent, causing no mortality after 30 h of bath immersion, similar to the control group (Fig. 1B). The impact of Ax 200 and Ax 198 on Pa virulence was then evaluated. Pre-immersion with Ax 200 ($OD_{600} = 0.5$) prior to introducing Pa II.17 ($OD_{600} = 0.2$), significantly reduced embryo mortality, with 50% surviving beyond 30 hpi, compared to 100% mortality at 22 hpi when infected with Pa II.17 alone (Fig. 1B). In contrast, pre-immersion with Ax 198 ($OD_{600} = 0.5$) resulted in mortality levels comparable to those observed with Pa II.17 alone (Fig. 1B).

The proteome of *P. aeruginosa* Pa II.17 is more significantly impacted in co-culture with *A. xylosoxidans* Ax 200 than with Ax 198

When co-cultured with Ax 200, 623 Pa proteins out of the 2019 detected showed significant differential abundance compared to the Pa II.17 monoculture (p-value ≤ 0.05 and log2FC $|1|$, Fig. 2A, Supplementary Figs. S2A and S2B, Supplementary Tables S1 and S2). All of these proteins exhibited a log2 FC of less than -1, indicating a significant reduction in abundance during co-culture (Fig. 2A). In contrast, co-culture with Ax 198 resulted in only 35 out of 2216 detected proteins showing significant differential abundance (Fig. 2B, Supplementary Figs. S2A and S2B). Among these, only 13 proteins were similarly less abundant in both Ax 198-Pa II.17 and Ax 200-Pa II.17 co-cultures, suggesting distinct molecular mechanisms underlying the interactions between Pa II.17 and the two Ax strains. Proteins with significant changes in abundance in co-cultures were predominantly classified into categories "Translation, ribosomal structure and biogenesis", "Energy production and conversion" and "Amino acid transport and metabolism". Several were also grouped into the "Unknown function" category (Supplementary Fig. S2B). Notably, the latter included key proteins, such as PelC and AlgZ, involved in EPS biosynthesis, and the outer membrane porin OprD, known for its roles in the transport of amino acids and the uptake of antibiotics[15].

Some Pa II.17 proteins were also exclusively detected either in mono- or co-culture (Supplementary Fig. S2C), the majority of them (99.4% and 72%) being exclusively detected in the Pa monoculture and absent in the Ax 200-Pa II.17, or the Ax 198-Pa II.17 co-culture, respectively (Supplementary Tables S1 and S2).

By combining the proteins with differential abundance and those exclusively detected in either mono- or co-culture, the total number of Pa proteins impacted was 1936 for the co-culture with Ax 200 and 831 for the co-culture with Ax 198. Notably, only 410 of these 831 proteins (49.3%) overlapped with those affected in the Ax 200-Pa II.17 co-culture, further highlighting distinct interaction mechanisms (Supplementary Tables S1 and S2).

Altogether, Ax 200 exerts a more pronounced negative impact on Pa II.17 proteome, potentially affecting Pa growth, proliferation, metabolism, and most likely, virulence to a greater extent than Ax 198; and molecular interactions between Pa II.17 and Ax 200 are mechanistically distinct from those with Ax 198. The following sections focus on the main Pa virulence factors inhibited by Ax.

Biofilm formation and swimming motility in *P. aeruginosa* Pa II.17 is severely impaired in co-culture with *A. xylosoxidans* Ax 200

Key Pa virulence proteins were underrepresented or absent in the presence of Ax 200. Specifically, T4P proteins, including PilG, PilU, PilM, FimL, and FimV, were at least three times less abundant in Ax 200-Pa II.17 co-culture compared to Pa monoculture (Fig. 3, Supplementary Table S1). As T4P is essential for twitching motility[16–19], this suggests that Pa adhesion may be impaired during co-culture. In addition, PelC, involved in EPS production, was four times less abundant in co-culture (Fig. 3). As EPS secretion contributes to biofilm structural integrity, later stages of biofilm formation could also be negatively impacted by Ax 200. Moreover, FleQ, the master regulator of biofilm formation, was nearly 14 times less abundant in co-culture, further supporting that biofilm

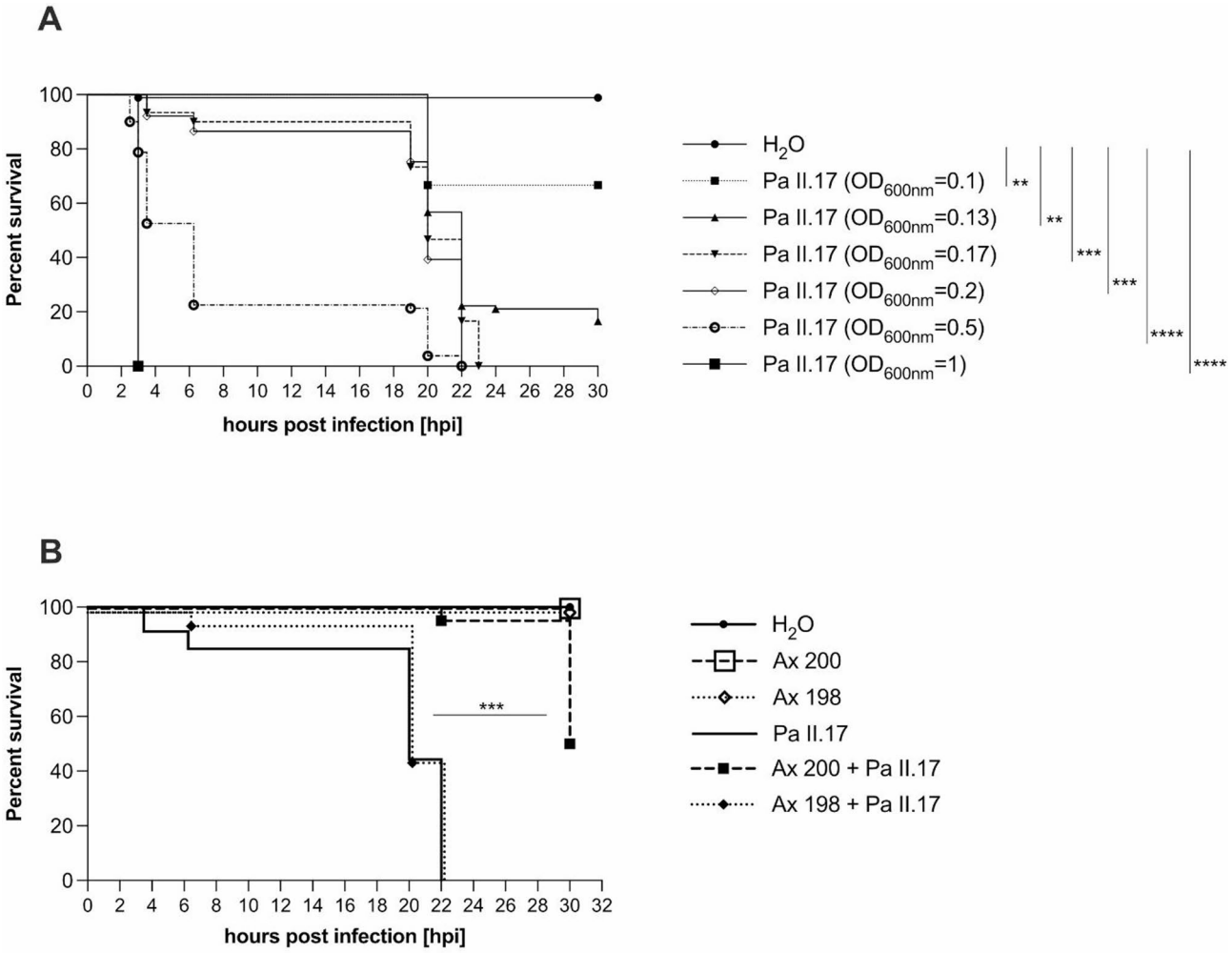

Fig. 1. Survival outcomes in the zebrafish infection model with Pa II.17 alone (**A**) or co-infections with Ax 200 or Ax 198 (**B**). Survival of zebrafish embryos at 48 h post-fertilization is represented as a Kaplan–Meier plot. (**A**) Zebrafish embryos were infected by bacterial suspensions of Pa II.17 at different concentrations (OD_{600} of 0.1, 0.13, 0.17, 0.2, 0.5 and 1, corresponding to concentrations ranging from 3×10^8 to 4×10^9 CFU/mL). The experiment was performed in five independent experiments and in three experiments for the highest dose ($OD_{600} = 1$). (**B**) Zebrafish embryos were infected by bacterial suspensions of either Pa II.17 (prepared in fish water at an OD_{600} of 0.2 corresponding to approximately 8×10^8 CFU/mL), Ax 200 (prepared in fish water at an OD_{600} of 0.5 corresponding to approximately 1×10^9 CFU/mL) or Ax 198 (prepared in fish water at an OD_{600} of 0.5 corresponding to approximately 1×10^9 CFU/mL) strains alone, or with Ax 200 or Ax 198 preincubation of 1.5 h before Pa II.17 introduction. The Ax 200–Pa II.17 co-infection experiment was conducted in three independent experiments, and the Ax 198–Pa II.17 co-infection experiment was conducted in two independent experiments under the same conditions. Embryos maintained in fish water were used as negative control. For each experiment, the optical density of each bacterial suspension was systematically measured before being distributed into the wells and Colony-forming units (CFUs) were estimated retrospectively from the inoculum suspensions. Results are presented as the proportion of surviving embryos ($n > 20$ for each, indicative of at least two separate experiments). Significant differences tested by log-rank test are indicated (**, $P \leq 0.01$; ***, $P \leq 0.001$; ****, $P \leq 0.0001$).

formation could be defective. Also, other proteins associated with biofilm regulation, such as SiaB, or with T4P formation such as PilT, PilB and PilD, were exclusively detected in Pa mono-culture (Fig. 3). To validate whether biofilm formation was indeed impaired by Ax 200, a biofilm formation assay was conducted. Consistent with our proteomic analysis, *in vitro* biofilm biomass of both strains combined was two times lower in Ax 200-Pa II.17 co-culture compared to biofilm formed in Pa monoculture (Fig. 4A).

Pa II.17 swimming motility which is crucial for both the initial adhesion phase and the dissemination of biofilms[20] is likely to be also impacted by Ax 200, as flagellar proteins were found to be 1.7 to 2.2 times less abundant in co-culture (Fig. 3). These include FlgL, which is inserted in the hook-filament junction; and the filament flagellin FliC. Several other proteins related to flagellum formation or function were detected only in

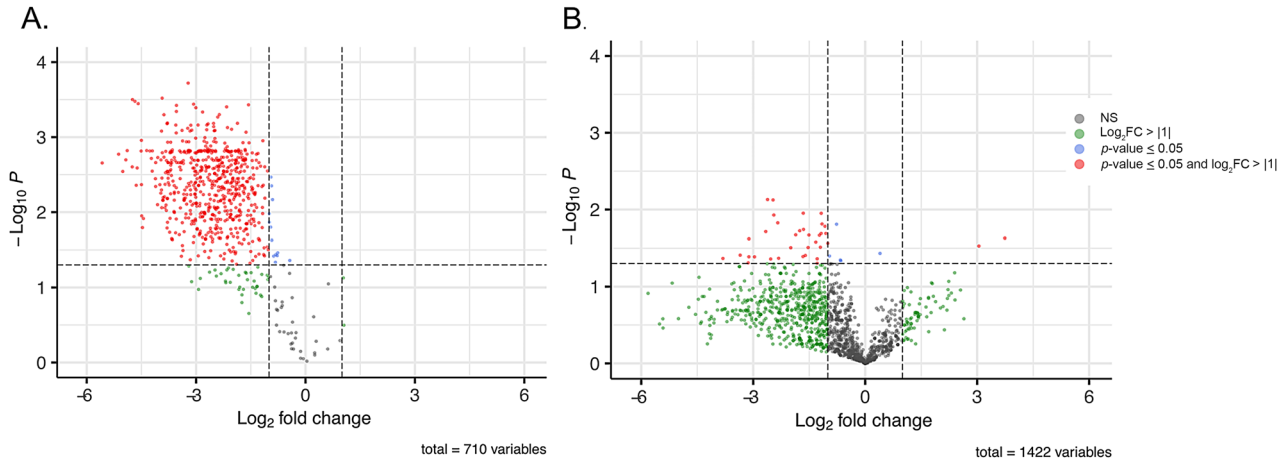

Fig. 2. *P. aeruginosa* Pa II.17 proteins displaying differential abundance between mono-culture and co-culture with *A. xylosoxidans* Ax 200 (**A**) or *A. xylosoxidans* Ax 198 (**B**). Each dot in the Volcano Plot represents a protein identified both in mono- and co-culture. Each mono- and co-cultures was analysed in triplicate. Changes in protein abundance were considered statistically significant (red dots) when the *p*-value was ≤ 0.05 (Student's *t*-test, horizontal dashed line) and the log2 FC exceeded |1|. NS = not significant.

Pa II.17 monoculture (Fig. 3). A motility assay confirmed that swimming was significantly reduced by 1.22-fold in co-culture compared to monoculture, consistent with the reduced abundance of flagellar proteins (Fig. 4B).

Iron uptake by *P. aeruginosa* is impaired in co-culture with *A. xylosoxidans* Ax 200

The ferric uptake regulator protein Fur, which is essential for maintaining iron homeostasis, was seven times less abundant in Ax 200-Pa II.17 co-culture compared to Pa monoculture (Fig. 3, Supplementary Table S1). Additionally, the pyochelin receptor FptA and another siderophore receptor were exclusively detected in Pa monoculture (Supplementary Table S1). These proteins display a signal peptide for secretion and are thus potentially secreted[21]. Iron uptake in Pa II.17 might thus be negatively affected by the presence of Ax 200, prompting further investigation in optimal conditions for assessing siderophore production impairments, *i.e.*, using the iron-depleted medium MM9[22]. In this condition, total siderophore production was reduced by nearly half in the co-culture (Fig. 4C) and pyoverdine production, one of the primary Pa siderophores, was also drastically reduced (Fig. 4D).

Abundance of secretion system proteins is reduced in *P. aeruginosa* co-cultured with *A. xylosoxidans* Ax 200

Proteins associated with the Type III secretion system (T3SS), such as PopB, a translocator protein essential for pore formation; PcrH, a chaperone stabilizing effector protein; and ExsC, a scaffold protein involved in T3SS assembly, were less abundant in co-culture with Ax 200. Additionally, numerous other structural and regulatory proteins of T3SS were exclusively detected in monoculture (Fig. 3, Supplementary Table S1). A protein associated with the Type II secretion system (T2SS) was also less abundant in co-culture, suggesting a reduced efficiency of T2SS in the presence of Ax 200. Similarly, the Type VI secretion system (T6SS) was significantly impacted, with several proteins detected only in monoculture, indicating impaired assembly or function of T6SS in co-culture (Fig. 3, Supplementary Table S1). Interestingly, VgrG2 was the only T6SS-protein found exclusively in co-culture and not in monoculture. However, the underrepresentation of other essential T6SS components in co-culture suggests a compromised functionality of T6SS in the presence of Ax 200.

Proteomic changes are limited in *P. aeruginosa* co-cultured with Ax 198, but key virulence phenotypes are still affected

In contrast to Ax 200, the presence of Ax 198 in co-culture with Pa II.17 did not significantly reduce the abundance of proteins involved in biofilm, T4P or TSS system functionality (Fig. 3). Indeed, only FimL, a central regulator required for T4P biogenesis, biofilm development, and T3SS function, was less abundant in Ax 198-Pa II.17 co-culture compared to Pa monoculture. This suggested that specific Pa phenotypes could still be affected in the presence of Ax 198. Phenotypic assays revealed that biofilm formation by Pa II.17 was significantly reduced in co-culture with Ax 198 (Fig. 4A). This reduction might also be explained by the absence or reduction of several proteins exclusively detected in Pa monoculture, including SiaB and PelC for biofilm regulation; PopN and PscR for T3SS; and LcmF2, ClpV2, Hcp and HsiC2 for T6SS (Fig. 3, Supplementary Table S2).

Regarding the abundance of QS proteins, none of the changes detected between Pa monoculture and Ax 198-Pa II.17 co-culture were statistically significant in our conditions. However, some QS proteins such as the acyl-homoserine lactone (AHL) synthetase LasI, and third QS system proteins PqsB and PqsE, were not detected in Ax 198-Pa II.17 co-culture (Supplementary Table S2). Overall, QS proteins exhibited greater alterations in the Ax 198-Pa II.17 co-culture compared to Ax 200, where no differences were observed between mono- and co-culture.

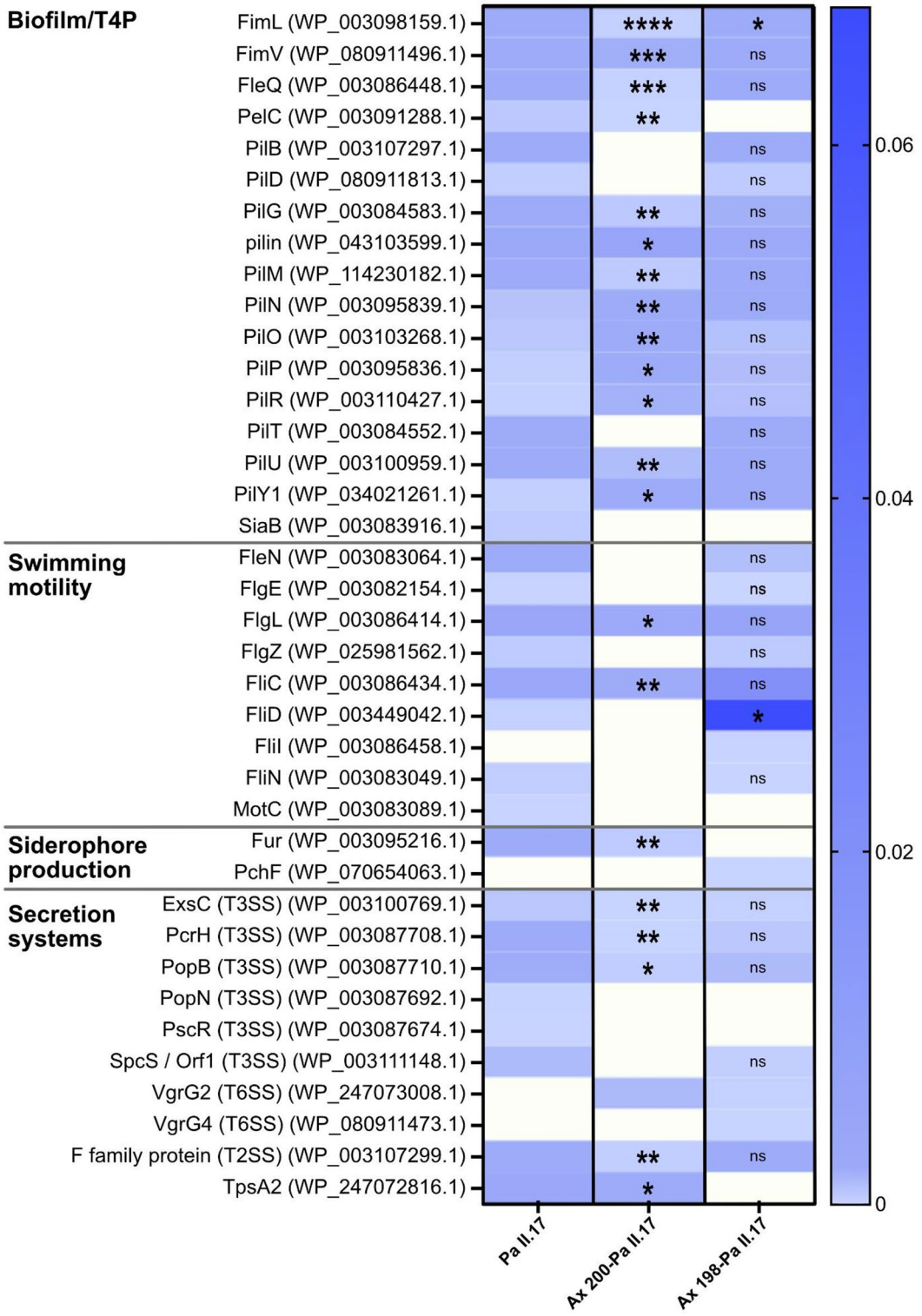

Fig. 3. Abundance of *P. aeruginosa* Pa II.17 virulence-associated proteins in monoculture and co-culture with *A. xylosoxidans* Ax 200 or Ax 198. Protein annotations were verified using BLASTp. Accession numbers are indicated in parentheses. Shades of blue indicate the average Normalized Spectral Abundance Factor (NSAF) of three replicates. Only proteins with a significant difference in abundance between mono- and co-culture and proteins exclusively detected either in mono- or co-culture are shown. The statistical significance of abundance variation between Pa II.17 mono-culture and Ax 200-Pa II.17 or Ax198 -Pa II.17 co-culture was assessed using a Student *t*-test; ****, $P \leq 0.0001$; ***, $P \leq 0.001$; **, $P \leq 0.01$; *, $P \leq 0.05$; ns = not significant. Blank cells indicate proteins not detected for which no statistical test was performed.

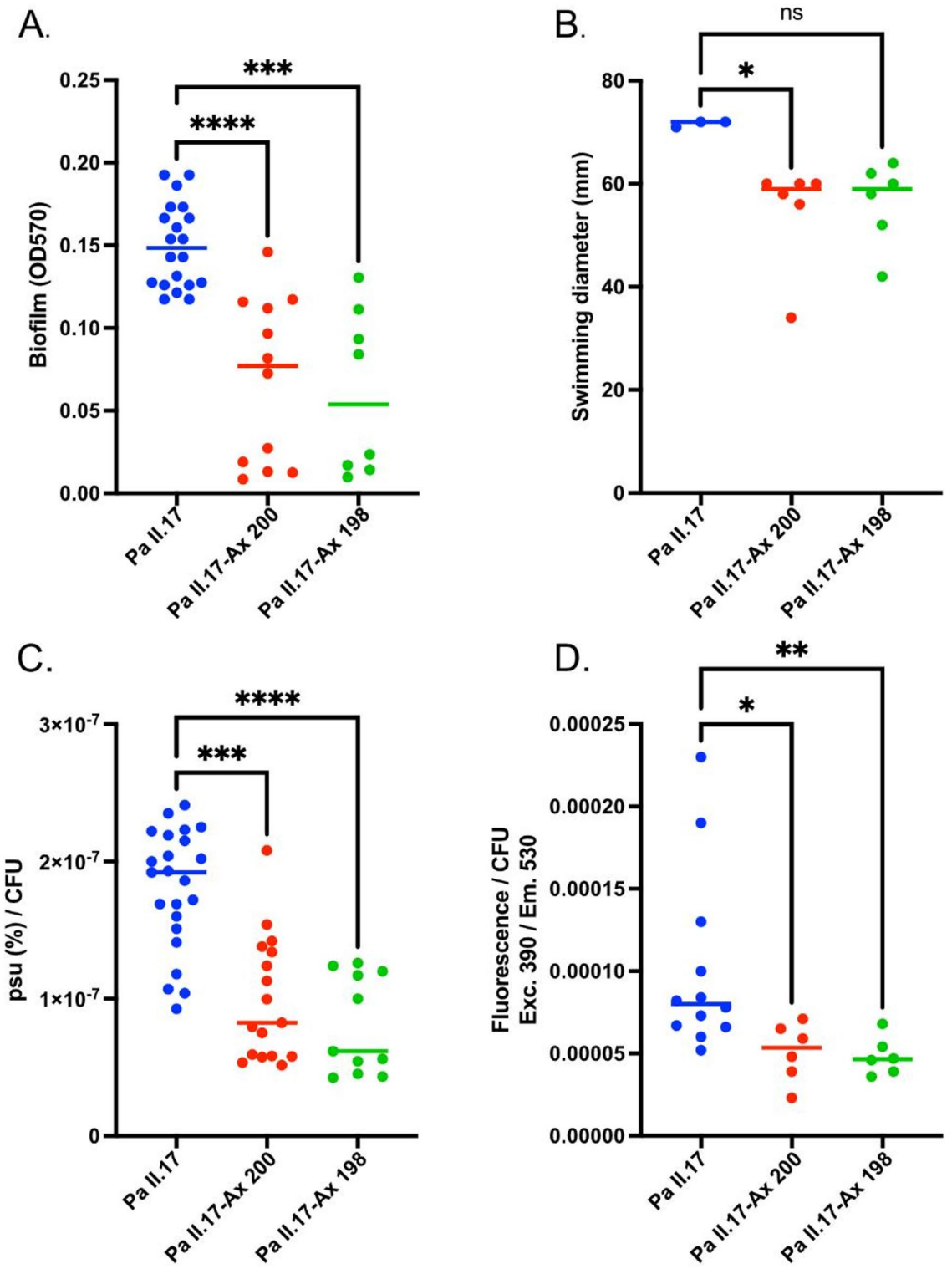

Fig. 4. Biofilm formation (**A**), swimming motility (**B**), siderophore production (**C**) and pyoverdine production (**D**) of *P. aeruginosa* Pa II.17 in monoculture and co-culture with *A. xylosoxidans* Ax 200 or Ax 198. The values are medians. The results of phenotypic tests were normalized across assays using the average result of each assay. Siderophore production was normalized on total CFU since Ax and Pa are both able to produce siderophores. Pyoverdine production was normalized exclusively on Pa CFU. The statistical significance of the results was calculated by a nonparametric Kruskal-Wallis test, ****, $P \leq 0.0001$; ***, $P \leq 0.001$; **, $P \leq 0.01$; *, $P \leq 0.05$; ns = not significant.

Regarding swimming motility, only FliD, a flagellar cap protein, was more abundant in Ax 198-Pa II.17 compared to monoculture (Fig. 3). This overabundance alone is unlikely to enhance swimming motility. In addition, three flagellar structural proteins, FlgG, FlaG and FliI, were detected exclusively in Ax 198-Pa II.17 co-culture (Supplementary Table S2), suggesting potentially more efficient flagellar formation. Nonetheless, phenotypic assays showed no significant differences in swimming motility for Ax 198-Pa II.17 co-culture compared to monoculture (Fig. 4B). This could be explained by the absence of essential regulators or structural proteins, such as FliH, FliS, MotC and FlgN, which were not detected in co-culture (Supplementary Table S2).

Concerning iron acquisition, siderophore production in Ax 198-Pa II.17 co-culture was significantly reduced compared to monoculture, similar to the reduction observed with Ax 200 (Fig. 4C). Notably, proteomic data highlighted distinct profiles between the two conditions. For example, while Fur was less abundant in co-cultures with Ax 198 or Ax 200, PchF, required for pyochelin biosynthesis, was only detected in Ax 198-Pa II.17 co-culture (Fig. 3).

Genetic basis for differential effects of *A. xylosoxidans* Ax 198 and Ax 200 on *P. aeruginosa* virulence

Sixty variations, either single nucleotide polymorphisms (SNPs) or deletions/insertions, were identified between the Ax 200 and Ax 198 genomes, of which 37 were located in coding sequences corresponding to 31 genes (Supplementary Table S3). Most of these genes encode proteins of "unknown function", while the remaining genes encode proteins primarily involved in transcription (Supplementary Fig. S3). Based on Bakta and Prokka annotations, SNPs were identified in three genes encoding transcriptional regulators: *dmlR*, *nusA* and a tetR-type helix-turn-helix (HTH) domain-containing protein-encoding gene (Supplementary Table S3). The corresponding transcriptional regulators regulate pyruvate metabolism, transcript elongation, and tetracycline resistance, respectively. Additionally, five SNPs were identified in the *yqjI* gene of Ax 200, leading to the loss of a start codon and subsequent absence of functional YqjI protein production (Supplementary Table S3). YqjI, a PadR family transcriptional regulator, is known to control the transcription of *yqjH* in *Escherichia coli*[23], which encodes the ferric reductase YqjH, a key enzyme promoting reduction of Fe^{3+} and its release from siderophores in the cytoplasm. Furthermore, a SNP was found in the ferripyoverdine receptor FhuE-encoding gene between the Ax 198 and Ax 200 genomes. Also, in the Ax 200 genome, a SNP caused the loss of a stop codon in a porin-encoding gene, suggesting a potentially dysfunctional porin. Notably, no SNPs were detected in genes encoding TSS components or regulators. These findings suggest that distinct regulatory pathways, including those related to iron metabolism, contribute to the differences in Ax-Pa competition between Ax 198 and Ax 200.

Discussion

As lung infections in CF patients are considered polymicrobial[24], investigating interbacterial competition and its effects on virulence is particularly relevant. Although the major CF pathogen Pa is increasingly exposed to Ax during polymicrobial lung infection in CF patients[25], the most frequently isolated species[26,27], the interaction between these two species remains poorly understood.

The colonization and persistence of Pa in the respiratory tract rely on its remarkable versatility including transitioning from a planktonic motile lifestyle during host invasion to biofilm formation, enabling immune evasion and antimicrobial resistance[28]. This transition is tightly regulated by the intracellular second messenger c-di-GMP and its receptor-effector, FleQ, a master transcriptional regulator. In response to high c-di-GMP, FleQ represses flagellar biosynthesis and activates EPS production genes (*psl*, *pel*, *cdr*AB), enhancing biofilm formation by inhibiting swimming motility and promoting matrix production[29–31]. FleQ detected in Pa II.17 proteome was significantly reduced in co-culture with Ax 200, likely altering the transcription of FleQ-dependent genes[30]. Moreover, an essential feature of the initial stage of Pa biofilm development is surface adhesion *via* twitching motility[32], mediated by T4P extension and retraction[33]. PilG and PilU, key T4P proteins[16,34], were significantly less abundant in the Pa II.17 proteome during co-culture with Ax 200 likely contributing to the observed reduction in biofilm formation. By uncovering the molecular basis for the reduction of biofilm in co-culture, we demonstrated that Ax 200 not only impairs biofilm formation (from initial adhesion and matrix production to dissemination *via* swimming motility) but also disrupts the planktonic-to-sessile transition, thereby limiting Pa adaptive capacity. The PilSR two-component system is known to regulate swimming motility in Pa as it has been shown that pilSR deletion mutants lead to swimming defects[35]. This two-component system could be involved in our case, as PilR was more abundant in the presence of Ax 200. T4P is also a critical adhesin facilitating host epithelial cell colonization[18]. The reduced abundance of T4P structural and functional proteins in Ax 200-Pa II.17 co-culture likely contributes to diminished host cell infection, as evidenced by the lower zebrafish mortality observed during co-infection. Therefore, our study validates and extends the findings of two previous studies that reported reductions in biofilm formation and motility *in vitro* for this strain pair and other Ax-Pa combinations[13,14]. By incorporating *in vivo* experiments and proteomic analyses, our work goes beyond these earlier studies, providing deeper insights into the molecular basis underlying these phenotypic changes and demonstrating their relevance in a host infection model. Also, zebrafish is widely recognized as a relevant and powerful model for studying CF pathogens[36].

Secretion systems are key virulence factors of Pa[18,37]. FimL is a central regulator required not only for T4P activity and biofilm development, but also for the functionality of T3SS that enables Pa to inject effectors into host cells, disrupting their machinery, inducing cytotoxicity, and enhancing bacterial survival[38]. Our findings showed that FimL was less abundant in Pa when co-cultured with Ax 200, and as expected, the T3SS-associated proteins were also less represented. This is the first report of T3SS disruptions during Ax-Pa interactions. *P. aeruginosa* possesses four other TSSs[37]. T2SS was also affected in Ax-Pa co-culture with several T2SS-related proteins being less abundant in co-culture. T2SS + Pa strains are known to cause lethal infections in mice, albeit more slowly than T3SS + strains[39]. Finally, T6SS, known to mediate Pa internalization into eukaryotic cells *via*

effectors such as Vgr2[40], was significantly impaired, indicating that Ax 200 disrupts T6SS functionality in Pa during co-culture.

The Pa virulence arsenal also includes siderophores secreted to facilitate iron uptake[41], which is essential for numerous cellular processes. During infection, Pa competes with the host and microbial species for iron, relying on two siderophores, pyoverdine and pyochelin, which are critical for establishing successful infections[8,42]. For example, siderophores are central to the interplay between the two main CF pathogens, Pa and *S. aureus*, as they are required for Pa to kill *S. aureus* efficiently[43,44]. However, no prior studies have reported the involvement of iron homeostasis or siderophore production in interactions between Pa and *Achromobacter.* Here, we observed that siderophore production by Pa II.17 was significantly reduced when co-cultured with Ax 200. Since Ax is also capable of producing siderophores[45], it was initially unclear which microorganism was responsible for this decrease. However, by measuring pyoverdine, we confirmed that Pa was at least partially responsible for the observed siderophore reduction. Moreover, Pa has more than 30 receptors that recognize its own siderophores as well as xenosiderophores produced by other bacteria, facilitating their transport into the cells[46]. Our proteomic analyses revealed that at least two receptors, including the pyochelin receptor FptA, were detected in Pa monoculture only, suggesting that under our experimental conditions where iron was not limited, Pa iron uptake might be less effective in the presence of Ax 200. Similarly, the Fur regulator, critical for iron homeostasis, was significantly less abundant in the presence of Ax 200[47,48]. This is the first study to report the involvement of iron homeostasis and siderophore production in Ax-Pa interactions, suggesting that Ax interference with Pa iron acquisition strategies may be a key factor in attenuating Pa virulence. Supporting this hypothesis, we found that the ferrireductase regulator-encoding gene *yqjI* was mutated in the Ax 200 genome.

Altogether, this study highlights a multi-target mechanism of competition between Ax and Pa, whereby Ax simultaneously disrupts multiple Pa virulence factors. The potential impact of proteases secreted by Ax[49–51] on the degradation—and thus the reduction—of certain Pa proteins remains to be explored. This finding challenges the prevailing view of Pa as a highly competitive species that outcompete other species[52,53]. Moreover, the patient colonization history, marked by chronic Ax colonization and sporadic Pa presence, raises questions about the role of bacterial competition in shaping infection outcomes[54]. The involvement of such interactions in the success of colonizers in CF patients, as well as their potential consequences on patients' clinical status and management, remains to be elucidated. Examining the effect of Pa on the Ax proteome could provide further insights into these dynamics.

Our findings reveal that interaction between Pa and Ax is strain-dependent, likely driven by distinct mechanisms specific to each strain. For instance, QS regulation may play a role in the interaction with Ax 198 but not with Ax 200. A previous study on strains isolated from the same patient at different infection stages has also described varied interactions between Pa and Ax, ranging from coexistence and competition[14]. Our study is the first to report distinct types of interaction between Pa and Ax strains co-isolated from the same sputum sample, highlighting how adaptive microevolution in CF lungs can generate sub-clonal co-existing Ax variants with differing competitive abilities against Pa. Such diversity within the Ax population likely provides an adaptive advantage, enabling the population to respond to environmental changes, including new colonization episodes by opportunistic pathogens like Pa, and supporting the long-term survival of Ax in CF lungs[54–57]. Although the study of two differentially adapted Ax strains, both isolated from the same patient, was a strength for understanding the specific interactions between Ax and Pa, this may also limit a broader applicability of our findings to other patients or strain combinations. Regarding underlying mechanisms, the most notable genomic variations between Ax 198 and Ax 200 were related to transcriptional regulators, iron uptake, and porin genes. In addition, QS regulation may play a role in the interaction with Ax 198 but not with Ax 200. Our findings also excluded that defective TSSs in Ax 198 explain its lesser impact on Pa virulence. Indeed, both Ax 198 and Ax 200 carry genes encoding T6SS, T2SS and T3SS, as well as components of T1SS and T4SS, as reported in CF Ax strains[50,58,59] and no significant differences in TSS-related genomic regions, including those related to transcriptional, post-transcriptional, or post-translational regulators, were found between both genomes[60]. This contrasts with previous studies demonstrating that Ax T6SS could target and kill the Pa reference strain PAO1[61] and that T6SS VgrG and T1SS components were encoded by a competitive *Achromobacter* strain and absent in a co-existing strain[14].

Methods

Patient, bacterial strains and ethical statement

Pa II.17, Ax 198 and Ax 200 were co-isolated from a sputum sample obtain from a CF patient attending the CF center at Montpellier University Hospital, France. The patient was chronically colonized by Ax and sporadically colonized by Pa (Supplementary Fig. 2 in [13]). Ax 198 and Ax 200 are clonally-related according to previous genotyping, including *nrdA* gene sequencing, Multi-Locus Sequence Typing, Pulsed-Field Gel Electrophoresis and Multiplex rep-PCR[13]. The study was conducted according to the guidelines of the Declaration of Helsinki. Ethical approval was obtained through the Institutional Review Board at Nîmes University hospital (Interface Recherche Bioéthique number 19.02.01) for this observational study that fell into the category of routine practice with non-additional diagnostic and monitoring procedures applied to the patient and retrospective analysis of primary data derived from routine clinical care. Informed consent was obtained from subject involved in the study.

Bath immersion-based zebrafish embryo survival assay and ethical statement

Overnight (O/N) bacterial cultures grown at 37 °C in Trypticase Soy Broth (TSB) were centrifuged at 3500 g for 10 min and resuspended in fish water (distilled water with 60 µg/mL sea salt, Instant Ocean, and 4.10^{-4} N NaOH). Bacterial suspensions were adjusted to an optical density of 600 nm (OD_{600}), with bacterial counts verified by plating on Tryptic Soy Agar (TSA). Experiments were conducted in fish water at 28 °C using the

zebrafish model (*Danio rerio*) (AB zebrafish line). Embryos were dechorionated at 48 h post-fertilization (hpf) and infected *via* bath immersion. Groups of 10 healthy embryos were placed in 6-well plates containing the bacterial suspension. For pre-incubation, fish water was replaced either by 2 mL of Ax suspension (OD_{600} = 1.0) or by 2 mL of fish water (for Pa-only conditions). After 1.5 h, 2 mL of Pa suspension—prepared at twice the desired final OD_{600}—was added to the wells. In conditions where Ax was incubated alone, 2 mL of fish water was added instead, ensuring comparable final bacterial concentrations across conditions. Dead embryos were visually identified by the absence of a heartbeat.

All experiments were performed in accordance with European Union guidelines for the care and use of laboratory animals (http://ec.europa.eu/environment/chemicals/labanimals/homeen.htm) and were approved by the Direction Sanitaire et Vétérinaire de l'Hérault and the Comité d'Ethique pour l'Expérimentation Animale (CEEA-LR-13007). At the end of experiments, plates were sealed with parafilm, frozen at − 20 °C for 48 h to ensure the embryo's death, and autoclaved.

Mono- and co-culture conditions

Overnight cultures in TSB were used to inoculate mono-cultures (Ax 198, Ax 200, or Pa II.17) or co-cultures (Ax 198-Pa II.17 or Ax 200-Pa II.17) in specific media, depending on the experiment. To account for Ax's slower growth rate compared to Pa, co-culture conditions followed the protocol of Menetrey *et al.*[13]. Briefly, Ax was inoculated first at OD_{600} = 0.005, followed by Pa inoculation at OD_{600} = 0.001 after a 4 h delay. After 48 h of incubation at 37 °C, the cultures were used for proteomic analysis or phenotypic assays. A 48-hour incubation was chosen based on our previous study[13] in which Ax 200, continue to grow significantly between 24 h and 48 h (approximately one log increase), both in monoculture and in co-culture with Pa. Since a significant proportion of the bacterial population may consist of dead cells after 48 h, we performed bacterial counts to assess viable bacteria only. Bacterial cell counts (CFU/mL) were determined using TSA plates and the EasySpiral Pro (Interscience®) system, following the manufacturer's instructions. Pa and Ax colonies were visually distinguished.

Proteomic analysis

For each condition (Pa II.17-Ax 198 or Pa II.17-Ax 200 co-culture, Pa II.17 mono-culture in two independent assays), proteome extraction was performed as described previously[62]. Cultures were centrifugated at 3000 g for 15 min at 20 °C; pellets were resuspended in 1 ml of PBS 1X pH 7.0 (Sigma-Aldrich), centrifuged at 10,000 g for 3 min, and subsequently dissolved in 100 µL LDS 1X supplemented with 5% β-mercaptoethanol. Secreted proteins were analyzed after trichloroacetic acid (TCA) (Sigma-Aldrich) precipitation of the culture supernatants, and since most exoproteins were recovered in proteome due to cell lysis, the results from both fractions were combined for analysis. Peptides were analysed using an ESI-Q Exactive HF mass spectrometer (ThermoFisher Scientific) coupled with an Ultimate 3000 Nano LC System (ThermoFisher Scientific). Peptides were quantified, and the peptide volume to be injected for each sample was normalized accordingly. Peptides were injected onto a reverse phase Acclaim PepMap 100 C18 column (3 µm, 100 Å, 75 µm id × 500 mm) and resolved at 0.2 µL/min with a 90-min gradient of CH_3CN (4–40%) containing 0.1% HCOOH. The tandem mass spectrometer operated in data-dependent mode using a top-20 strategy, selecting peptide molecular ions with double or triple positive charges for fragmentation, with a 10 s dynamic[63].

The tandem mass spectrometry (MS/MS) spectra were interpreted using MASCOT Daemon 2.6.0 software (Matrix Science) with genomes of Ax 200, Ax 198, and Pa II.17 (accession numbers GCA_022976495.1, GCA_022976515.1, and GCA_022976545.1, respectively). Parameters included full-trypsin specificity, a maximum of one missed cleavage, 5 ppm mass tolerance on parent ions, and 0.02 Da on MS/MS. Modifications considered were carbamidomethylated cysteine as a static modification and oxidized methionine as a dynamic modification. Peptides with MASCOT scores below a *p*-value of 0.05 were included.

Proteins quantification was based on spectral counts using the Normalized Spectral Abundance Factor (NSAF)[64]. Each condition included three biological replicates. Proteins were considered detected if MS/MS-assigned spectra were counted in at least two of these replicates. Fold change was calculated as the NSAF ratio of co-cultures to the summed NSAF of Pa mono-cultures. Statistical significance of abundance variation between mono- and co-culture was assessed using a Student *t*-test. Proteins with statistically non-significant results, or inconsistent abundances between two independent Pa mono-cultures were excluded. Functional annotation of detected proteins was conducted using the eggNOG v5 database[65].

Quantification of siderophore and pyoverdine production

Mono- and co-cultures were performed in minimal medium MM9 (0.3 g/L KH_2PO_4, 0.5 g/L NaCl, 0.1 g/L NH_4Cl supplemented with 3.3% Casamino acid, 0.2% glucose, 1 mM $MgCl_2$, 100 µM $CaCl_2$ and 7.5 mg/L tryptophan) under static conditions according to Payne's method with modifications[66]. Siderophore production was assessed using the universal Chrome Azurol Sulphonate (CAS) assay[66,67]. Briefly, after 48 h at 37 °C, 80 µL of supernatants were mixed with 80 µL of CAS reagent. Absorbance at 630 nm was measured after 5 min. Siderophore production was expressed as percent siderophore units (psu) calculated using the formula: [(Ar - As)/Ar]100 = % siderophore units, where Ar represents the absorbance of the reference (CAS solution and uninoculated broth) and As represents the absorbance of the sample (CAS solution with the supernatant). To quantify pyoverdine production, 100 µL of culture supernatants were transferred to black 96-well plates wells (Greiner) and fluorescence was measured at excitation/emission wavelengths of 390 nm/530 nm using a multimode microplate reader (TECAN, spark)[68].

Results were normalized by dividing the data obtained by the CFU count for each sample to take into account the interaction effect on Pa growth of co-culture with Ax, as described previously[13] and confirmed herein (Supplementary Fig. S4). Each assay was performed in triplicate and repeated at least twice. Following

confirmation of data normality with the Shapiro-Wilk test, statistical significance was determined using nonparametric Kruskal-Wallis test.

Quantification of biofilm formation

Biofilm formation was assessed as described previously[13]. Briefly, O/N cultures were used in the biofilm formation assays performed in 96-well plates, with an initial OD_{600} of 0.005 for Ax strains and 0.001 for Pa. For dual-species assays (Ax 198-Pa II.17 and Pa II.17- Ax 200), bacterial suspensions were prepared in TSB from O/N cultures to obtain a final $OD_{600} = 0.005$ for Ax strains and $OD_{600} = 0.001$ for Pa strains (taking into account the two-fold dilution of 50 µL of each suspension in the 1:1 ratio mix). Biofilm quantification was performed after 48 h of incubation at 37 °C based on Harvey *et al.*[69], with modifications[13]. The wells were washed thrice with tap water and stained with 1% crystal violet (CV) solution. The CV was then solubilized using 200 µL of 95% ethanol, and 125 µL of the solution was transferred to a new plate for absorbance measurement at 570 nm. Data normality was verified using the Shapiro-Wilk test, and statistical analyses were conducted using one-way analysis of variance (ANOVA).

Swimming motility assays

Swimming motility was assessed following a modified protocol from Menetrey *et al.*[13]. A 2.5 µL aliquot of Ax 198 or Ax 200 suspension at $OD_{600} = 0.5$ was inoculated into the swim plates (20 g/L Luria Bertani broth, 0.3% agar). After 4 h of incubation at 30 °C, a 2.5 µL aliquot of Pa II.17 suspension at $OD_{600} = 0.1$ was inoculated 1.5 cm away from the Ax spot. Plates were incubated at 30 °C for an additional 44 h. Pa swimming ability was evaluated by measuring the diameter of the turbid circular zone and comparing it to the zone formed by Pa when cultured alone. All experiments were performed in triplicate.

Whole genome sequencing and comparison of *Achromobacter* genomes

Bacterial DNA was extracted using the MasterPure extraction kit (Epicentre) and sequenced on an Illumina NextSeq 500 at the Plateforme de Microbiologie Mutualisée (P2M, Institut Pasteur, Paris, France). Reads were assembled *de novo* using SPAdes v3.12.0[70]; contigs were annotated *via* the NCBI Prokaryotic Genome Annotation Pipeline (PGAP)[71]. Ax genome alignments were visualized using BRIG. Sequence Types (ST) were determined *via* the PubMLST database (https://pubmlst.org). Both substitutions and insertions/deletions (indels) between *Achromobacter* genomes were identified using Snippy v4.6.0 (https://github.com/tseemann/snippy), with core genome SNPs (Single Nucleotide Polymorphisms) determined using Snippy-core. These tools were run on the Galaxy platform[72] with default settings. Functional annotation of SNPs-associated genes was conducted using the eggNOG v5 public database[65]. Average Nucleotide Identity by BLAST was calculated using the JSpecies webserver (http://jspecies.ribohost.com/jspeciesws)[73], while digital DNA–DNA hybridization was estimated with GGDC 3.1[74].

Data availability

Mass spectrometry proteomic data have been deposited in the ProteomeXchange Consortium *via* the PRIDE[75] partner repository with the dataset identifiers PXD058911 and 10.6019/PXD058911. Raw genome sequencing data and assemblies were deposited in GenBank under the BioProject accession numbers PRJNA823997 and PRJNA824006. A preliminary version of this manuscript was deposited on bioRxiv and is available at https://doi.org/10.1101/2025.02.26.640371.

Received: 28 February 2025; Accepted: 5 June 2025
Published online: 02 July 2025

References

1. Mena, K. D. & Gerba, C. P. Risk assessment of *Pseudomonas aeruginosa* in water. *Rev. Environ. Contam. Toxicol.* **201**, 71–115 (2009).
2. Crone, S. et al. The environmental occurrence of *Pseudomonas aeruginosa*. *APMIS* **128**, 220–231 (2020).
3. Lamas Ferreiro, J. L. et al. Fernández *Pseudomonas aeruginosa* urinary tract infections in hospitalized patients: Mortality and prognostic factors. *PLoS One* **12**, e0178178 (2017).
4. Motbainor, H., Bereded, F. & Mulu, W. Multi-drug resistance of blood stream, urinary tract and surgical site nosocomial infections of *Acinetobacter baumannii* and *Pseudomonas aeruginosa* among patients hospitalized at Felegehiwot referral hospital, Northwest ethiopia: a cross-sectional study. *BMC Infect. Dis.* **20**, 92 (2020).
5. Garau, J. & Gomez, L. *Pseudomonas aeruginosa* pneumonia. *Curr. Opin. Infect. Dis.* **16**, 135–143 (2003).
6. van Delden, C. *Pseudomonas aeruginosa* bloodstream infections: how should we treat them? *Int. J. Antimicrob. Agents*. **30** (Suppl 1), S71–S75 (2007).
7. Foundation, C. F. Cystic Fibrosis Foundation Patient Registry 2022 Annual Data Report. (2022).
8. Morin, C. D., Déziel, E., Gauthier, J., Levesque, R. C. & Lau, G. W. An organ system-based synopsis of *Pseudomonas aeruginosa* virulence. *Virulence* **12**, 1469–1507 (2021).
9. Sibley, C. D. & Surette, M. G. The polymicrobial nature of airway infections in cystic fibrosis: cangene gold medal lecture. *Can. J. Microbiol.* **57**, 69–77 (2011).
10. O'Brien, T. J. & Welch, M. Recapitulation of polymicrobial communities associated with cystic fibrosis airway infections: a perspective. *Future Microbiol.* **14**, 1437–1450 (2019).
11. Parkins, M. D. & Floto, R. A. Emerging bacterial pathogens and changing concepts of bacterial pathogenesis in cystic fibrosis. *J. Cyst. Fibros.* **14**, 293–304 (2015).
12. Tetart, M. et al. Impact of *Achromobacter xylosoxidans* isolation on the respiratory function of adult patients with cystic fibrosis. *ERJ Open. Res.* **5**, 00051–2019 (2019).
13. Menetrey, Q., Dupont, C., Chiron, R., Jumas-Bilak, E. & Marchandin, H. High occurrence of bacterial competition among clinically documented opportunistic pathogens including *Achromobacter xylosoxidans* in cystic fibrosis. *Front. Microbiol.* **11**, 558160 (2020).

14. Sandri, A. et al. Adaptive interactions of *Achromobacter* spp. With *Pseudomonas aeruginosa* in cystic fibrosis chronic lung co-infection. *Pathogens* **10**, 978 (2021).
15. Yoneyama, H. & Nakae, T. Mechanism of efficient elimination of protein D2 in outer membrane of imipenem-resistant *Pseudomonas aeruginosa*. *Antimicrob. Agents Chemother.* **37**, 2385–2390 (1993).
16. Bertrand, J. J., West, J. T. & Engel, J. N. Genetic analysis of the regulation of type IV pilus function by the chp chemosensory system of *Pseudomonas aeruginosa*. *J. Bacteriol.* **192**, 994–1010 (2010).
17. Ayers, M. et al. PilM/N/O/P proteins form an inner membrane complex that affects the stability of the *Pseudomonas aeruginosa* type IV pilus secretin. *J. Mol. Biol.* **394**, 128–142 (2009).
18. Whitchurch, C. B. et al. *Pseudomonas aeruginosa* FimL regulates multiple virulence functions by intersecting with Vfr-modulated pathways. *Mol. Microbiol.* **55**, 1357–1378 (2005).
19. Wehbi, H. et al. The peptidoglycan-binding protein FimV promotes assembly of the *Pseudomonas aeruginosa* type IV pilus secretin. *J. Bacteriol.* **193**, 540–550 (2011).
20. Khong, N. Z. et al. Dynamic swimming pattern of *Pseudomonas aeruginosa* near a vertical wall during initial attachment stages of biofilm formation. *Sci. Rep.* **11**, 1952 (2021).
21. Teufel, F. et al. SignalP 6.0 predicts all five types of signal peptides using protein Language models. *Nat. Biotechnol.* **40**, 1023–1025 (2022).
22. Murugappan, R. M., Aravinth, A., Rajaroobia, R., Karthikeyan, M. & Alamelu, M. R. Optimization of MM9 medium constituents for enhancement of siderophoregenesis in marine *Pseudomonas putida* using response surface methodology. *Indian J. Microbiol.* **52**, 433–441 (2012).
23. Wang, S., Wu, Y. & Outten, F. W. Fur and the novel regulator YqjI control transcription of the ferric reductase gene YqjH in *Escherichia coli*. *J. Bacteriol.* **193**, 563–574 (2011).
24. Peters, B. M., Jabra-Rizk, M. A., O'May, G. A., Costerton, J. W. & Shirtliff, M. E. Polymicrobial interactions: impact on pathogenesis and human disease. *Clin. Microbiol. Rev.* **25**, 193–213 (2012).
25. Veschetti, L. et al. *Achromobacter* spp. Prevalence and adaptation in cystic fibrosis lung infection. *Microbiol. Res.* **263**, 127140 (2022).
26. Firmida, M. C. et al. *Achromobacter xylosoxidans* infection in cystic fibrosis siblings with different outcomes: case reports. *Respir Med. Case Rep.* **20**, 98–103 (2017).
27. Spilker, T., Vandamme, P. & LiPuma, J. J. Identification and distribution of *Achromobacter* species in cystic fibrosis. *J. Cyst. Fibros.* **12**, 298–301 (2013).
28. Moser, C. et al. Immune responses to *Pseudomonas aeruginosa* biofilm infections. *Front. Immunol.* **12**, 625597 (2021).
29. Hickman, J. W. & Harwood, C. S. Identification of FleQ from *Pseudomonas aeruginosa* as a c-di-GMP-responsive transcription factor. *Mol. Microbiol.* **69**, 376–389 (2008).
30. Oladosu Victoria, I., Park, S. & Sauer, K. Flip the switch: the role of FleQ in modulating the transition between the free-living and sessile mode of growth in *Pseudomonas aeruginosa*. *J. Bacteriol.* **206**, e00365–e00323 (2024).
31. Baraquet, C. & Harwood, C. S. FleQ DNA binding consensus sequence revealed by studies of FleQ-dependent regulation of biofilm gene expression in *Pseudomonas aeruginosa*. *J. Bacteriol.* **198**, 178–186 (2016).
32. O'Toole, G. A. & Kolter, R. Flagellar and twitching motility are necessary for *Pseudomonas aeruginosa* biofilm development. *Mol. Microbiol.* **30**, 295–304 (1998).
33. Burrows, L. L. *Pseudomonas aeruginosa* twitching motility: type IV pili in action. *Annu. Rev. Microbiol.* **66**, 493–520 (2012).
34. Buensuceso, R. N. C. et al. Cyclic AMP-independent control of twitching motility in *Pseudomonas aeruginosa*. *J. Bacteriol.* **199**, e00188–e00117 (2017).
35. Kilmury, S. L. N. & Burrows, L. L. The *Pseudomonas aeruginosa* PilSR two-component system regulates both twitching and swimming motilities. *mBio* 9. (2018).
36. Bernut, A., Loynes, C. A., Floto, R. A. & Renshaw, S. A. Deletion of Cftr leads to an excessive neutrophilic response and defective tissue repair in a zebrafish model of sterile inflammation. *Front. Immunol.* **11**, 1733 (2020).
37. Filloux, A. Protein secretion systems in *Pseudomonas aeruginosa*: an essay on diversity, evolution, and function. *Front. Microbiol.* **2**, 155 (2011).
38. Horna, G. & Ruiz, J. Type 3 secretion system of *Pseudomonas aeruginosa*. *Microbiol. Res.* **246**, 126719 (2021).
39. Jyot, J. et al. Type II secretion system of *Pseudomonas aeruginosa*: in vivo evidence of a significant role in death due to lung infection. *J. Infect. Dis.* **203**, 1369–1377 (2011).
40. Sana, T. G. et al. Internalization of *Pseudomonas aeruginosa* strain PAO1 into epithelial cells is promoted by interaction of a T6SS effector with the microtubule network. *mBio* **6**, e00712 (2015).
41. Ghssein, G. & Ezzeddine, Z. A review of *Pseudomonas aeruginosa* metallophores: pyoverdine, pyochelin and pseudopaline. *Biology (Basel)*. **11**, 1711 (2022).
42. Takase, H., Nitanai, H., Hoshino, K. & Otani, T. Impact of siderophore production on *Pseudomonas aeruginosa* infections in immunosuppressed mice. *Infect. Immun.* **68**, 1834–1839 (2000).
43. Filkins, L. M. et al. Coculture of *Staphylococcus aureus* with *Pseudomonas aeruginosa* drives *S. aureus* towards fermentative metabolism and reduced viability in a cystic fibrosis model. *J. Bacteriol.* **197**, 2252–2264 (2015).
44. Limoli, D. H. et al. *Pseudomonas aeruginosa* alginate overproduction promotes coexistence with *Staphylococcus aureus* in a model of cystic fibrosis respiratory infection. *mBio* **8**. https://doi.org/10.1128/mbio.00186-17 (2017).
45. Sorlin, P. et al. Prevalence and variability of siderophore production in the *Achromobacter* genus. *Microbiol. Spectr.* **12**, e0295323 (2024).
46. Chan, D. C. K. & Burrows, L. L. *Pseudomonas aeruginosa* FpvB is a high-affinity transporter for xenosiderophores ferrichrome and Ferrioxamine B. *mBio* **14**, e0314922 (2023).
47. Hassett, D. J. et al. Ferric uptake regulator (Fur) mutants of *Pseudomonas aeruginosa* demonstrate defective siderophore-mediated iron uptake, altered aerobic growth, and decreased superoxide dismutase and catalase activities. *J. Bacteriol.* **178**, 3996–4003 (1996).
48. Pasqua, M. et al. Ferric uptake regulator Fur is conditionally essential in *Pseudomonas aeruginosa*. *J. Bacteriol.* **199**. (2017).
49. Veschetti, L., Sandri, A., Johansen, H. K., Lleò, M. M. & Malerba, G. Hypermutation as an evolutionary mechanism for *Achromobacter xylosoxidans* in cystic fibrosis lung infection. *Pathogens* **9** (2020).
50. Jakobsen, T. H. et al. Complete genome sequence of the cystic fibrosis pathogen *Achromobacter xylosoxidans* NH44784-1996 complies with important pathogenic phenotypes. *PLoS One*. **8**, e68484 (2013).
51. Li, X., Hu, Y., Gong, J., Zhang, L. & Wang, G. Comparative genome characterization of *Achromobacter* members reveals potential genetic determinants facilitating the adaptation to a pathogenic lifestyle. *Appl. Microbiol. Biotechnol.* **97**, 6413–6425 (2013).
52. Cheng, Y. et al. Population dynamics and transcriptomic responses of *Pseudomonas aeruginosa* in a complex laboratory microbial community. *NPJ Biofilms Microbiomes*. **5**, 1 (2019).
53. Shah, R. et al. *Pseudomonas aeruginosa* kills *Staphylococcus aureus* in a polyphosphate-dependent manner. mSphere 9. (2024).
54. Armitage, D. W. & Jones, S. E. How sample heterogeneity can obscure the signal of microbial interactions. *Isme J.* **13**, 2639–2646 (2019).
55. Menetrey, Q. et al. *Achromobacter xylosoxidans* and *Stenotrophomonas maltophilia*: emerging pathogens well-armed for life in the cystic fibrosis patients' lung. *Genes (Basel)* 12. (2021).

56. Dupont, C. et al. Intrapatient diversity of *Achromobacter* spp. Involved in chronic colonization of cystic fibrosis airways. *Infect. Genet. Evol.* **32**, 214–223 (2015).
57. Dupont, C., Jumas-Bilak, E., Michon, A. L., Chiron, R. & Marchandin, H. Impact of high diversity of *Achromobacter* populations within cystic fibrosis sputum samples on antimicrobial susceptibility testing. *J. Clin. Microbiol.* **55**, 206–215 (2017).
58. Ridderberg, W., Nielsen, S. M. & Nørskov-Lauritsen, N. Genetic adaptation of *Achromobacter* sp. during persistence in the lungs of cystic fibrosis patients. *PLoS One*. **10**, e0136790 (2015).
59. Jeukens, J. et al. A pan-genomic approach to understand the basis of host adaptation in *Achromobacter*. *Genome Biol. Evol.* **9**, 1030–1046 (2017).
60. Chen, L., Zou, Y., She, P. & Wu, Y. Composition, function, and regulation of T6SS in *Pseudomonas aeruginosa*. *Microbiol. Res.* **172**, 19–25 (2015).
61. Le Goff, M. et al. Characterization of the *Achromobacter xylosoxidans* type VI secretion system and its implication in cystic fibrosis. *Front. Cell. Infect. Microbiol.* **12**, 859181 (2022).
62. Durand, B. et al. Proteomic insights into *Helcococcus kunzii* in a diabetic foot ulcer-like environment. *Proteom. Clin. Appl.* **17**, e2200069 (2023).
63. Klein, G. et al. RNA-binding proteins are a major target of silica nanoparticles in cell extracts. *Nanotoxicology* **10**, 1555–1564 (2016).
64. Christie-Oleza, J. A., Fernandez, B., Nogales, B., Bosch, R. & Armengaud, J. Proteomic insights into the lifestyle of an environmentally relevant marine bacterium. *Isme J.* **6**, 124–135 (2012).
65. Huerta-Cepas, J. et al. EggNOG 5.0: a hierarchical, functionally and phylogenetically annotated orthology resource based on 5090 organisms and 2502 viruses. *Nucleic Acids Res.* **47**, D309–d314 (2019).
66. Payne, S. M. Detection, isolation, and characterization of siderophores. *Methods Enzymol.* **235**, 329–344 (1994).
67. Schwyn, B. & Neilands, J. B. Universal chemical assay for the detection and determination of siderophores. *Anal. Biochem.* **160**, 47–56 (1987).
68. Besse, A., Groleau, M. C., Trottier, M., Vincent, A. T. & Déziel, E. *Pseudomonas aeruginosa* strains from both clinical and environmental origins readily adopt a stable small-colony-variant phenotype resulting from single mutations in c-di-GMP pathways. *J. Bacteriol.* **204**, e0018522 (2022).
69. Harvey, J., Keenan, K. P. & Gilmour, A. Assessing biofilm formation by *Listeria monocytogenes* strains. *Food Microbiol.* **24**, 380–392 (2007).
70. Bankevich, A. et al. SPAdes: a new genome assembly algorithm and its applications to single-cell sequencing. *J. Comput. Biol.* **19**, 455–477 (2012).
71. Li, W. et al. RefSeq: expanding the prokaryotic genome annotation pipeline reach with protein family model curation. *Nucleic Acids Res.* **49**, D1020–D1028 (2021).
72. Community, G. The galaxy platform for accessible, reproducible, and collaborative data analyses: 2024 update. *Nucleic Acids Res.* **52**, W83–W94 (2024).
73. Richter, M., Rosselló-Móra, R., Oliver Glöckner, F. & Peplies, J. JSpeciesWS: a web server for prokaryotic species circumscription based on pairwise genome comparison. *Bioinformatics* **32**, 929–931 (2016).
74. Meier-Kolthoff, J. P., Carbasse, J. S., Peinado-Olarte, R. L. & Göker, M. TYGS and LPSN: a database tandem for fast and reliable genome-based classification and nomenclature of prokaryotes. *Nucleic Acids Res.* **50**, D801–D807 (2022).
75. Perez-Riverol, Y. et al. The PRIDE database resources in 2022: a hub for mass spectrometry-based proteomics evidences. *Nucleic Acids Res.* **50**, D543–d552 (2022).

Acknowledgements

The authors thank Teresa Sawyers, Medical Writer at the B.E.S.P.I.M., Nîmes University Hospital, for her assistance in editing this manuscript, and Corentin Escobar and Caroline Santer, for their contribution to preliminary zebrafish experiments and phenotypic assays.

Author contributions

Conceptualization: QM, VM, LG, HM. Data curation, Formal analysis, Investigation, Methodology, Validation: AB, QM, VJP, SHB, FA, CD, LG. Project administration, Supervision: HM. Resources: RC, EJB, JA, VM. Vizualisation: AB, QM. Writing: original draft: AB, QM, HM. Writing: review & editing: all authors.

Declarations

Competing interests

The authors declare no competing interests.

Additional information

Supplementary Information The online version contains supplementary material available at https://doi.org/10.1038/s41598-025-06075-w.

Correspondence and requests for materials should be addressed to A.B.